Temperature dependence of the cathodic and anodic kinetics in a copper electrowinning cell based on reactive electrodialysis

L. Cifuentes[a],[*], J. Simpson[b]

[a]*Departamento de Ingeniería de Minas, Universidad de Chile, Tupper 2069, Santiago, Chile*
[b]*Departamento de Ingeniería Metalúrgica, Universidad de Santiago, Av. Ecuador 3659, Santiago, Chile*

Abstract

The temperature dependence of various kinetic parameters for the copper electrodeposition reaction and for the ferrous to ferric ion oxidation has been experimentally determined. Potentiodynamic sweeps were carried out in a reactive electrodialysis cell in the 30–60 °C range in order to obtain expressions for each parameter as a function of temperature. In the conditions studied, for both reactions, the exchange current density depends on temperature as $\ln[i_0(\mathrm{A/m^2})] = -a/T + b$ and the limiting current density, as $|i_L(\mathrm{A/m^2})| = cT - d$. For the copper electrodeposition reaction, the charge transfer coefficient is constant, whereas for the ferrous to ferric ion oxidation it depends on temperature as $\alpha = fT^2 + gT + h$ (a–h are constants). These expressions can be used in a temperature-dependent model of a membrane-based copper electrowinning cell.

Keywords: Temperature; Chemical reactors; Kinetics; Electrochemistry; Membrane; Modeling

1. Introduction

1.1. Objectives

This work attempts to establish the temperature dependence of various kinetic parameters (charge transfer coefficient, exchange current density, limiting current density) for the main cathodic and anodic reactions in a reactive electrodialysis (RED) cell. This cell is made up of two compartments, the first one containing the cathode and the catholyte, and the second one containing the anode and the anolyte. The compartments are separated by an anion membrane meant to prevent cation transfer between the electrolytes. The cathodic reaction is copper electrodeposition and the anodic reaction is ferrous to ferric ion oxidation. At the operating cell current densities, both reactions take place under mixed control. The design and operation of this cell have been described in detail elsewhere (Cifuentes et al., 2004a,b).

The objectives of the present work are: (a) to study the effect of temperature on the exchange current density, the charge transfer coefficient and the limiting current density of the $Cu^{2+} + 2e \rightarrow Cu^0$ and $Fe^{2+} \rightarrow Fe^{3+} + e$ reactions and (b) to produce mathematical relationships for the temperature dependence of the said parameters which could help the development of a temperature-dependent RED cell model.

1.2. Calculation of kinetic parameters

The cell current density for a cathodic reaction under mixed control is given by

$$|i_c| = \frac{i_{0c}|i_{Lc}|}{i_{0c} + |i_{Lc}| \exp(\frac{\alpha_c F}{RT} \eta_c)} \tag{1}$$

and, for an anodic reaction under the same type of control,

$$i_a = \frac{i_{0a} i_{La}}{i_{0a} + i_{La} \exp(\frac{-\alpha_a F}{RT} \eta_a)}, \tag{2}$$

[*] Corresponding author. Tel.: +562 678 4510; fax: +562 672 3504.
  E-mail address: luicifue@ing.uchile.cl (L. Cifuentes).

where i_{0c}, i_{0a} are cathodic and anodic exchange current densities, A/m^2, i_{Lc}, i_{La} are cathodic and anodic limiting current densities, A/m^2, α_c, α_a are cathodic and anodic charge transfer coefficients, η_c, η_a are cathodic and anodic overpotentials, V, F is the Faraday's constant, 96 500 C/eq, R is gas constant, 8.314 J/mol K and T is temperature, K.

In order to determine the values of these parameters, potentiodynamic sweeps were carried out. These experiments provided data for $i = f(\eta)$ at various temperatures. The values of i_0, i_L and α for the copper electrodeposition reaction were obtained by the least-squares method (Chapra and Canale, 1998), i.e., by minimizing the expression

$$Z = \sum_{k=j}^{N} w_k \left[|i|_k - \frac{i_{0c}|i_{Lc}|}{i_{0c} + |i_{Lc}| \exp(\frac{\alpha_c F}{RT} \eta_{ck})} \right]^2. \tag{3}$$

The same parameters, for the ferrous to ferric ion oxidation, were obtained by minimizing the expression

$$Z = \sum_{k=j}^{N} w_k \left[|i|_k - \frac{i_{0a} i_{La}}{i_{0a} + i_{La} \exp(\frac{-\alpha_a F}{RT} \eta_{ak})} \right]^2. \tag{4}$$

In Eqs. (3) and (4): w_k is the weighting factor for each experimental point in the potentiodynamic sweep, N is number of data points, j is first data point in the mixed control range and k is kth data point in the potentiodynamic sweep.

These equations were solved by an adapted Newton–Raphson method (Chapra and Canale, 1998), producing i_0, i_L and α values for each studied temperature.

In the present work, 800 data points were captured for each sweep and the resulting data were processed by Excel software, first, in order to obtain parameter values at each studied temperature, and then to obtain expressions for each parameter as a function of temperature.

1.3. Previous work

There have been numerous studies of copper electrodeposition ($Cu^{2+} + 2e \rightarrow Cu^0$) kinetics (e.g., Andersen et al.,1973; Peykova et al., 1995; Zagorovskii et al., 2001; Vicenzo and Cavallotti, 2002; Cifuentes et al., 2004a). The values of the kinetic parameters (exchange current density, charge transfer coefficient and limiting current density) obtained by these authors vary with cell geometry and temperature, composition and hydrodynamics of the electrolyte; they also vary with the cathode materials used.

The ferrous to ferric ion oxidation ($Fe^{2+} \rightarrow Fe^{3+} + e$) has been chosen as an alternative to water decomposition ($2H_2O \rightarrow O_2 + 4H^+ + 4e$) in the design of new copper electrowinning cells because its use allows a drastic reduction in the cell voltage, from about 2 V (typical of conventional Cu electrowinning) to about 1 V (Sandoval, 1995; Cifuentes et al., 2004a). In addition, this reaction eliminates 'acid mist' and the produced ferric ion can be used as an oxidizing agent in combined leaching processes. The ferrous to ferric ion oxidation kinetics have also been studied by a number

of authors (e.g., Cooke et al., 1989; Lee, 1993; Rao et al., 1995; Sandoval et al., 1995; Das, 1996; Dew et al., 1985a,b; Jiricny and Evans, 1999; Marconi et al., 1996; Ronnholm et al. 1999a,b; Cifuentes et al., 2004a).

Various aspects of the design and operation of RED cells have been discussed by Cifuentes et al. (2004a,b). These cells have been shown to produce electrolytic copper at high values of the cell current density, cathodic current efficiency and specific energy consumption. A time-dependent model for the operation of a RED cell has been produced and validated (Cifuentes et al., 2004c). The test variables were copper production rate, ferric ion production rate, cell voltage as a function of time, catholyte and anolyte conductivities and specific energy consumption. The model was validated only for operation at 50 °C, therefore, further work is required to allow for model predictions at a range of temperatures. This work intends to advance towards this aim.

2. Experimental

Potentiodynamic sweeps were carried out at 30, 40, 50 and 60 °C (303, 313, 323 and 333 K) for both copper electrodeposition and ferrous to ferric ion oxidation. In order to approximate the conditions found in a RED copper electrowinning cell (cell geometry, electrolyte composition and hydrodynamics), the sweeps were conducted, for the cathodic reaction, in the cathode compartment of this cell and for the anodic reaction, in the anode compartment. In both cases, there was simultaneous catholyte and anolyte recirculation to ad hoc tanks. The experimental arrangements are shown in Figs. 1 and 2.

During normal operation of this cell, a current is generated by a rectifier and it is passed between anode and cathode. In the present case, anode, cathode and rectifier were absent, but the working, reference and counter electrodes depicted in Figs. 1 and 2 were connected to a Voltamaster 10 electrochemical interface in order to carry out the potentiodynamic sweeps.

In the copper electrodeposition case, the working electrode was a 1 cm $\times$ 1 cm $\times$ 0.05 cm electrolytic copper sheet and the counter electrode was a 2 cm $\times$ 2 cm $\times$ 0.01 cm platinum sheet. In the ferrous/ferric oxidation case, the working electrode was a 1 cm $\times$ 1 cm $\times$ 0.05 cm platinum sheet and the counter electrode was a 4 cm $\times$ 4 cm $\times$ 0.19 cm titanium mesh. In both cases, a saturated Hg_2SO_4/Hg reference electrode with Luggin capillary was used and the sweep rate was 0.5 mV/s.

The two-compartment RED cell was made of 15 mm thick acrylic plates held together by seven 5-mm diameter stainless steel bars bolted at both ends. Compartment dimensions were $7 \times 8.5 \times 1.4$ cm^3.

In both cases, the anolyte composition was 60 g/L Fe (from ferrous sulfate) and 190 g/L sulfuric acid. The catholyte composition was 30 g/L Cu (from cupric sulfate) and 190 g/L sulfuric acid. The source chemicals were
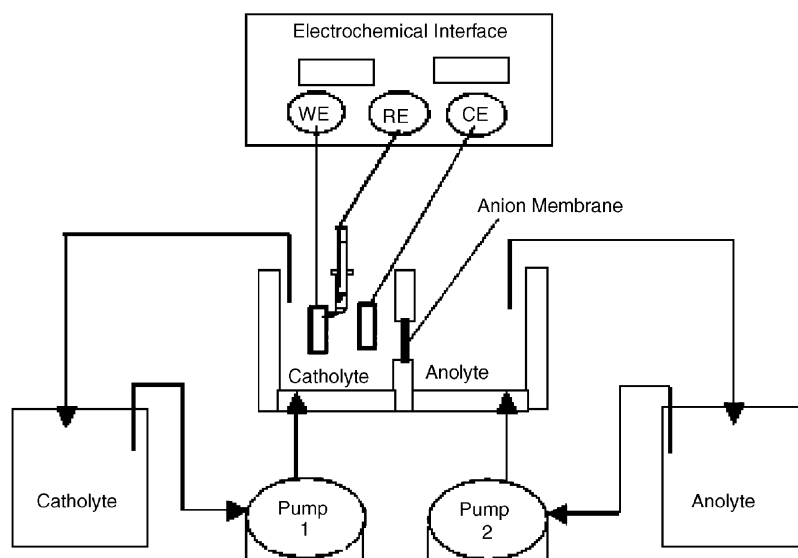
Fig. 1. Experimental arrangement for the study of the cathodic Cu^{2+}/Cu^0 reaction. WE = working electrode; RE = reference electrode; CE = counter electrode.
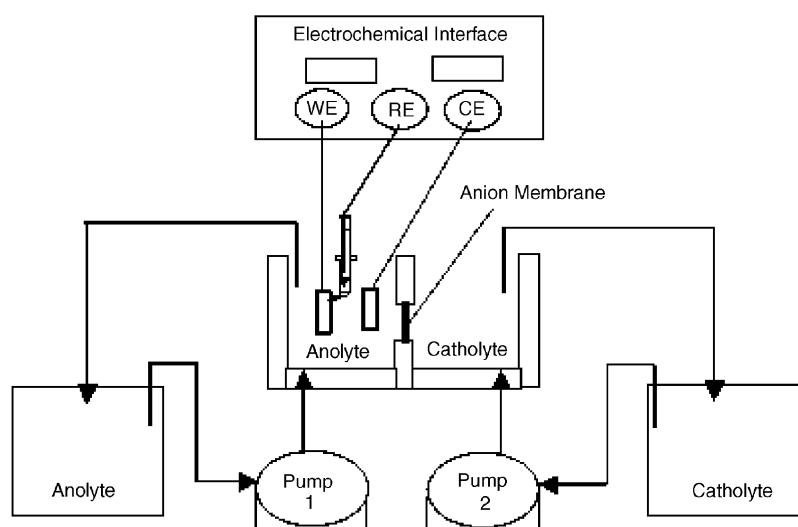

Fig. 2. Experimental arrangement for the study of the anodic Fe^{2+}/Fe^{3+} reaction. WE = working electrode; RE = reference electrode; CE = counter electrode.

analytical grade $CuSO_4 \cdot 5H_2O$, $FeSO_4 \cdot 7H_2O$ and 96% (w/w) sulfuric acid.

An Ionac MA-3475 anion membrane was used to separate anolyte from catholyte; it was fitted in a $4 \times 4 \, cm^2$ window cut in the acrylic plates between the compartments. This membrane was selected on the basis of availability and performance in previous works. It was kept in place by 2 mm thick rubber seals. Before each experiment, the membrane was pre-treated. Membrane properties and pre-treatment methods have been given elsewhere (Cifuentes et al., 2004b).

The electrolytes were separately recirculated at a flow rate of $700 \, cm^3/$ min, driven by two Cole-Parker WZIR051 peristaltic pumps. Two double-jacket, 1-L recirculation glass

tanks were used. The inner diameter of the recirculation inlet and outlet tubes fitted to the cell was 1 cm. Total volume for anolyte and catholyte was $600 \, cm^3$ each. The temperature of both electrolytes was kept constant during each experiment by a Julabo thermostatic bath.

3. Results and discussion

3.1. Cathodic kinetics

Cathodic kinetics in the mixed control range is represented in Fig. 3 as potentiodynamic curves at 30, 40, 50 and 60 °C. It is clear that, the higher the temperature, the higher
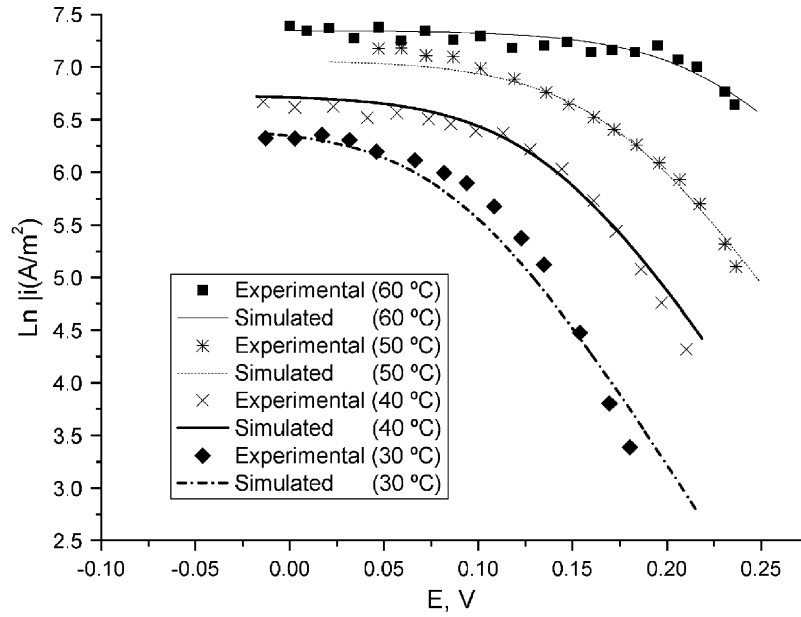
Fig. 3. Experimental and simulated potentiodynamic curves (ln |i| vs. E) for the cathodic Cu^{2+}/Cu^0 reaction at various temperatures.

Table 1
Kinetic parameters for the Cu^{2+}/Cu^0 reaction on a copper sheet cathode at various temperatures: a first approximation

Temperature (°C)	(K)	Exchange c. d. (i_0) (A/m^2)	Charge transfer coefficient (α_c)	Limiting c. d. (i_L) (A/m^2)
30	303	4.5	0.7440	614
40	313	19.6	0.7430	841
50	323	158.7	0.7429	1170
60	333	1268.2	0.7439	1351

the cathodic current density throughout the studied potential range.

The experimental curves in Fig. 3 were used to obtain a first approximation to the values for the kinetic parameters (i_0, α and i_L) from the procedure described in Section 1.2 above. These values are in Table 1. The simulated results in Fig. 3 are discussed below.

3.2. Cathodic charge transfer coefficient

Cathodic charge transfer coefficient (α_c) values from Table 1 are plotted against temperature in Fig. 4. α_c is practically constant in the studied temperature range. As this coefficient depends on the reaction mechanism, it becomes apparent that the mechanism for copper electrodeposition does not change with temperature in the studied range.

From these considerations, the cathodic charge transfer coefficient was assumed constant and it was calculated as the mean value from the results in Table 1, so, for the studied temperature range,

$$\alpha_c = 0.7434 \pm 0.0006. \tag{5}$$

The remaining parameters (i_{0c} and i_{Lc}) were recalculated by the procedure already described, but this time α_c was considered constant. These corrected (second approximation) parameters are given in Table 2.

Using the parameter values in Table 2 and an expression for the reaction rate under mixed control (Eq. (1)), simulated potentiodynamic sweeps were produced and plotted in Fig. 3. The simulated curves are in good agreement with experimental results.

3.3. Cathodic exchange current density

Various relationships between the exchange current density (i_0 in ampere per square meter) for the cathodic reaction and the absolute temperature (in Kelvin) were tried. A linear fit was found between the logarithm of the exchange current density (values in Table 2) and the reciprocal value of the absolute temperature. The plot is shown in Fig. 5.

The numerical relationship was obtained with Excel software as

$$\ln[i_{0c}(A/m^2)] = -20\,438\,\frac{1}{T(K)} + 68.33. \tag{6}$$

The correlation coefficient was 0.999.

This relationship is typical of mixed control given that, from Eq. (1):

$$\ln i_{0c} = -\frac{\alpha_c F |\eta_c|}{R}\frac{1}{T} + \ln\left|\frac{i_c i_{Lc}}{(i_c - i_{Lc})}\right| \tag{7}$$

and the latter expression exhibits the same form as Eq. (6) provided that the second term on the right-hand side of Eq. (7) remains fairly constant with temperature. Using experimental values for Eq. (7), as temperature increases from
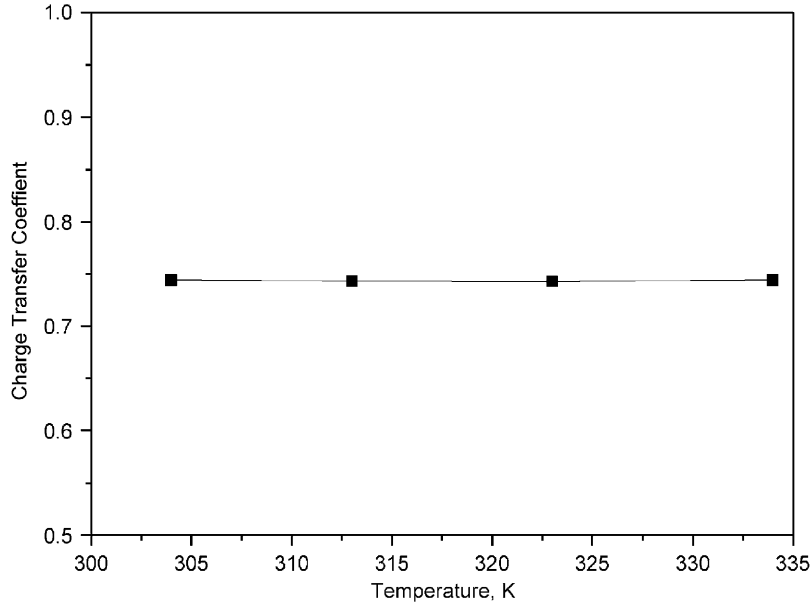
Fig. 4. Cathodic charge transfer coefficient (α_c) as a function of temperature for the Cu^{2+}/Cu^0 reaction.

Table 2
Kinetic parameters for the Cu^{2+}/Cu^0 reaction on a copper sheet cathode at various temperatures: a second approximation

Temperature (°C)	(K)	Exchange c. d. (i_0) (A/m^2)	Charge transfer coefficient (α_c)	Limiting c. d. (i_L) (A/m^2)
30	303	3.1	0.7434	616
40	313	19.6	0.7434	841
50	323	158.6	0.7434	1169
60	333	1268.8	0.7434	1269

30 to 60 °C, the first term on the right-hand side of the equation increases by about 60%, whereas the second term increases only by about 10%.

3.4. Cathodic limiting current density

The values of the limiting current density (i_{Lc} in ampere per square meter) for the cathodic reaction in Table 2 were plotted against the absolute temperature (Kelvin). The obtained relationship is linear (see Fig. 6) and it is given by

$$|i_{Lc}(A/m^2)| = 32.61\, T(K) - 9309.6. \tag{8}$$

The correlation coefficient was 0.986.

On the other hand, i_L can be calculated by Fick's equation as

$$i_L = zFD\frac{c_b}{\delta} = zFk_m c_b, \tag{9}$$

where c_b is the Ferrous ion concentration in the bulk solution, mol/m^3, D is diffusivity, m^2/s, k_m is mass transfer coefficient, m/s, and δ is thickness of the diffusion layer, m

In Fick's law, D, δ and k_m depend on temperature. The form of Eq. (8) suggests that

$$k_m(T) = \frac{D(T)}{\delta(T)} = aT - b, \tag{10}$$

where a and b are constants, because in this case, Fick's law becomes

$$|i_{Lc}| = zFc_b(aT - b) = zFc_b aT - zFc_b b \tag{11}$$

which exhibits the same form as Eq. (8).

3.5. Anodic kinetics

Anodic kinetics in the mixed control range are represented in Fig. 7 as potentiodynamic curves at 30, 40, 50 and 60 °C. The plots show that, the higher the temperature, the higher the anodic current density throughout the studied potential range.

The experimental curves in Fig. 7 were used to obtain the values for the kinetic parameters (i_0, α and i_L) from the procedure described in Section 1.2 above. These values are in Table 3. The simulated results were calculated with Eq. (2) and the parameter values in Table 3. There is good agreement between experiments and simulations.

3.6. Anodic charge transfer coefficient

Anodic charge transfer coefficient (α_a) values from Table 3 are plotted against temperature in Fig. 8. α_a varies with temperature. Considering that this coefficient depends on the reaction mechanism, it follows that the mechanism for ferrous to ferric ion oxidation changes with temperature in the studied range.
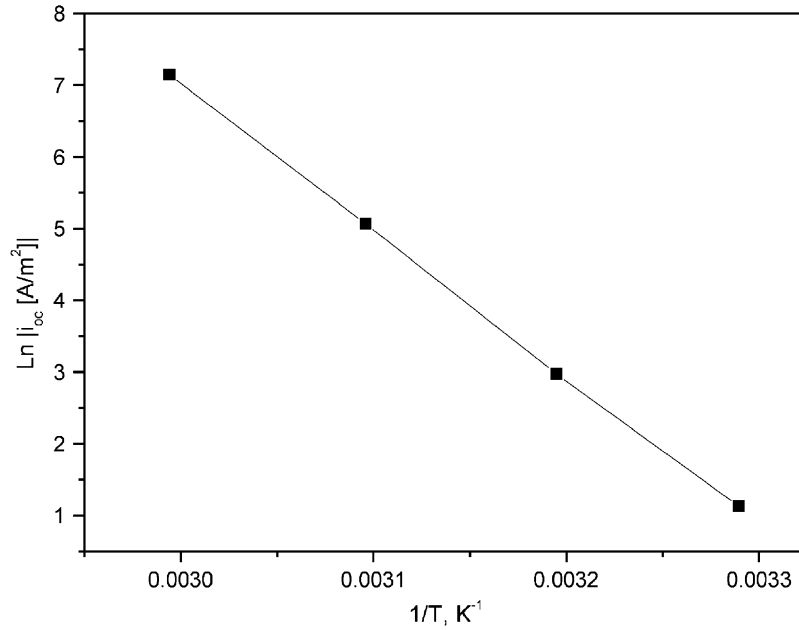
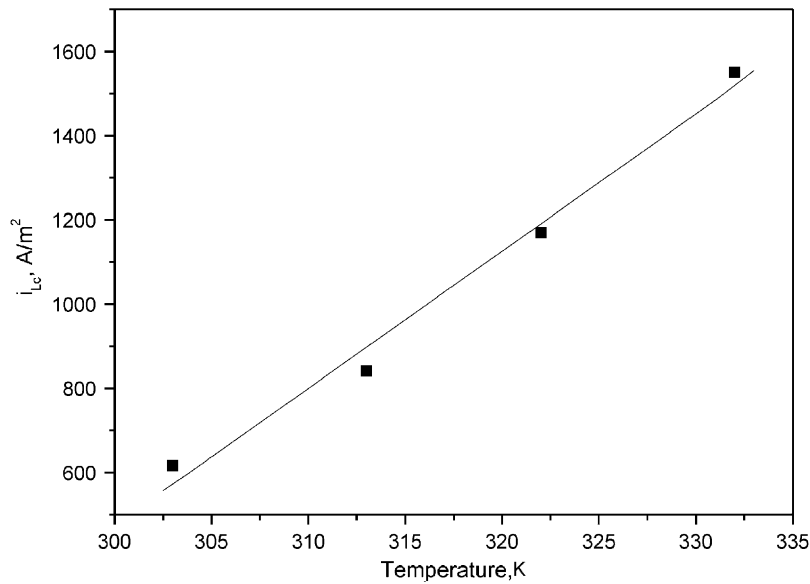Fig. 5. Logarithm of the exchange current density (i_{0c}) as a function of $1/T$ for the Cu^{2+}/Cu^0 reaction.

Fig. 6. Absolute value of the limiting current density ($|i_{Lc}|$) as a function of temperature for the Cu^{2+}/Cu^0 reaction.

The numerical relationship is

$$\alpha_a = 2 \times 10^{-4} \ T(K)^2 - 0.1113 \ T(K) + 17.385. \tag{12}$$

The correlation coefficient was 0.991. Further work is required in order to establish the reaction mechanisms involved.

3.7. Anodic exchange current density

Various relationships between the exchange current density (i_{0a} in ampere per square meter) for the anodic reaction and the absolute temperature (in Kelvin) were tried. As in the cathodic case, a linear fit was found between the logarithm of the exchange current density (values in Table 3) and the reciprocal value of the absolute temperature. The plot is shown in Fig. 9.

The numerical expression is

$$\ln[i_{0a}(A/m^2)] = -6403 \ \frac{1}{T(K)} + 23.828 \tag{13}$$

with a correlation coefficient of 0.996. It is of similar form to Eq. (6) and the considerations made in Section 3.3 also apply in this case.
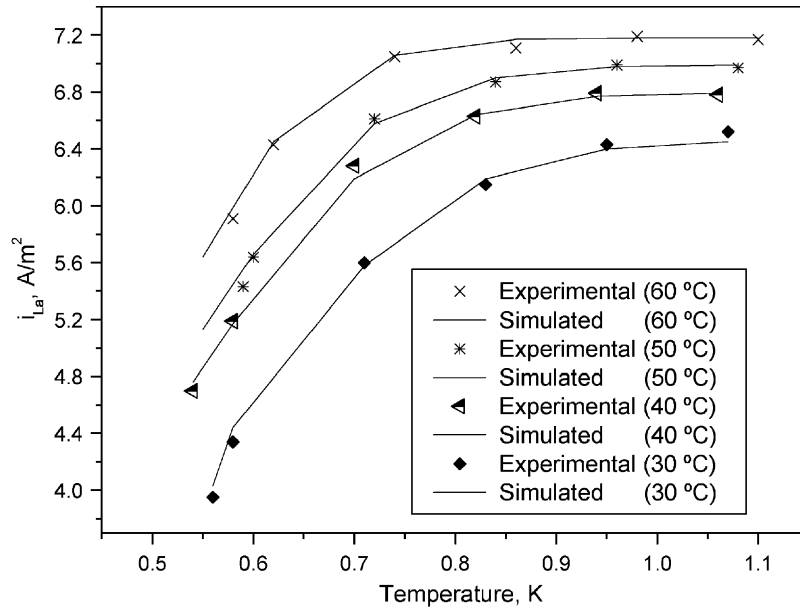
Fig. 7. Experimental and simulated potentiodynamic curves (ln |i| vs. E) for the anodic Fe^{2+}/Fe^{3+} reaction at various temperatures.

Table 3
Kinetic parameters for the Fe^{2+}/Fe^{3+} reaction on a platinum sheet anode at various temperatures

Temperature (°C)	(K)	Exchange c. d. (i_0) (A/m^2)	Charge transfer coefficient (α_c)	Limiting c. d. (i_L) (A/m^2)
30	303	15.4	0.3393	644
40	313	28.0	0.3534	901
50	323	49.3	0.3782	1091
60	333	98.3	0.4614	1317
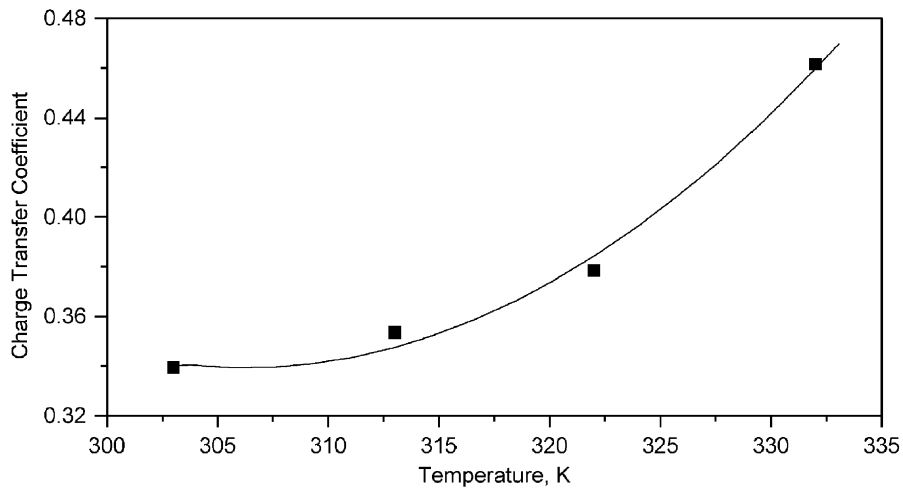
Fig. 8. Anodic charge transfer coefficient (α_a) as a function of temperature for the Fe^{2+}/Fe^{3+} reaction.

3.8. Anodic limiting current density

The values of the limiting current density (i_{La} in ampere per square meter) for the anodic reaction in Table 3 were plotted against the absolute temperature (Kelvin). The obtained relationship is linear (see Fig. 10)

and it is given by

$$i_{La}(A/m^2) = 23.015\ T(K) - 6318.9 \tag{14}$$

with a correlation coefficient of 0.998. This is similar to Eq. (8) and considerations put forward in Section 3.4 also apply here.
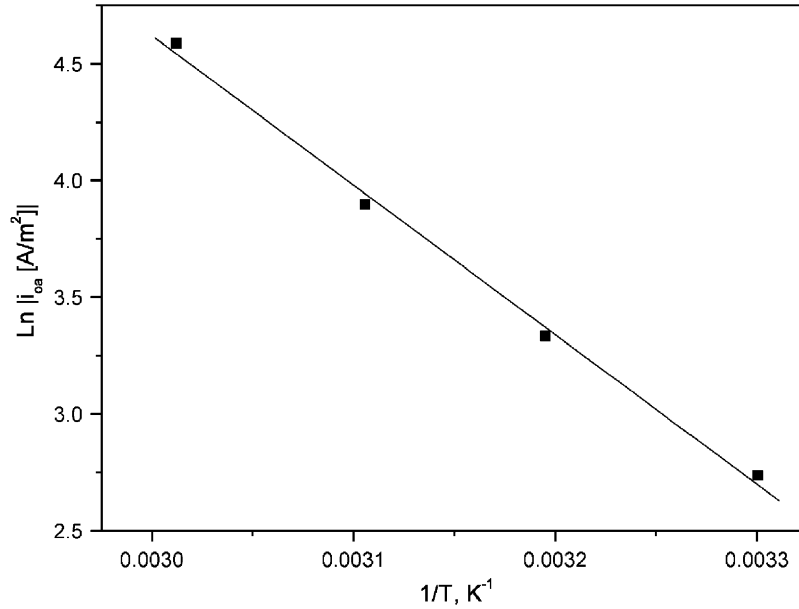
Fig. 9. Logarithm of the exchange current density (i_{0a}) as a function of $1/T$ for the Fe^{2+}/Fe^{3+} reaction.
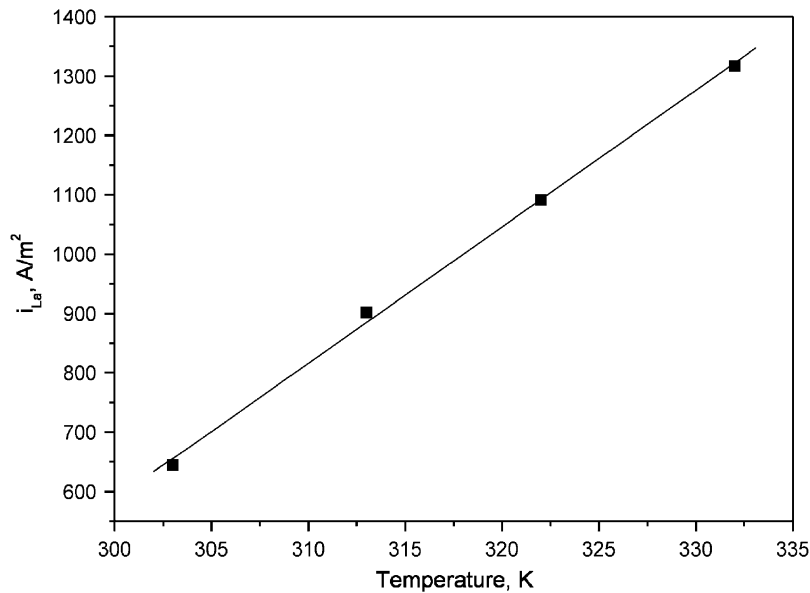

Fig. 10. Limiting current density (i_{La}) as a function of temperature for the Fe^{2+}/Fe^{3+} reaction.

The obtained relationships for all six kinetic parameters (α_c, i_{0c}, i_{Lc}, α_a, i_{0a} and i_{La}) as functions of temperature—Eqs. (5), (6), (8), (12), (13) and (14)—can be included in a temperature-dependent model for the operation of a membrane-based copper electrowinning cell.

4. Conclusions

In the 30–60 °C temperature range:

(1) Using the kinetic parameter values obtained from the experimental potentiodynamic sweeps and mixed control expressions for the calculation of both the cathodic and anodic reaction rates, gives good agreement between experiment and simulation.

(2) The charge transfer coefficient for the Cu^{2+}/Cu^0 reaction does not significantly change with temperature and its value is

$$\alpha_c = 0.7434 \pm 0.0006.$$

(3) The exchange current density for the Cu^{2+}/Cu^0 reaction depends on temperature as

$$\ln[i_{0c}(\text{A/m}^2)] = -20\,438\,\frac{1}{T\,(\text{K})} + 68.33.$$

(4) The limiting current density for the Cu^{2+}/Cu^0 reaction depends on temperature as

$$|i_{Lc}(A/m^2)| = 32.61\, T(K) - 9309.6.$$

(5) The charge transfer coefficient for the Fe^{2+}/Fe^{3+} reaction depends on temperature as

$$\alpha_a = 2 \times 10^{-4}\, T(K)^2 - 0.1113\, T(K) + 17.385.$$

(6) The exchange current density for the Fe^{2+}/Fe^{3+} reaction depends on temperature as

$$\ln[i_{0a}(A/m^2)] = -6403\,\frac{1}{T(K)} + 23.828.$$

(7) The limiting current density for the Fe^{2+}/Fe^{3+} reaction depends on temperature as

$$i_{La}(A/m^2) = 23.015\, T(K) - 6318.9.$$

(8) All these results can be used in a temperature-dependent mathematical model for the operation of the RED cell.

References

Andersen, T.N., Wright, C.N., Richards, K.J., 1973. Important electrochemical aspects of electrowinning copper from acid leach solutions. In: Evans, D.J.I., Shoemaker, R.S. (Eds.), International Symposium on Hydrometallurgy. AIME, New York, pp. 171–202.

Chapra, S.C., Canale, R.P., 1998. Numerical Methods for Engineers with Programming and Software Applications. McGraw-Hill, New York.

Cifuentes, L., Glasner, R., Casas, J.M., 2004a. Aspects of the development of a copper electrowinning cell based on reactive electrodialysis. Chemical Engineering Science 59, 1087–1101.

Cifuentes, L., Mondaca, C., Casas, J.M., 2004b. The effectiveness of membrane systems for the separation of anolyte and catholyte in a lab-scale copper electrowinning cell based on reactive electrodialysis. Minerals Engineering 17, 803–809.

Cifuentes, L., Castro, J.M., Crisóstomo, G., Casas, J.M., Simpson, J., 2004c. Modeling a copper electrowinning cell based on reactive electrodialysis. Submitted for publication.

Cooke, A.V., Chilton, J.P., Fray, D.J., 1989. Mass-transfer kinetics of the ferrous–ferric electrode process in copper sulphate electrowinning electrolytes. Transactions of the Institution of Mining and Metallurgy. Section C: Mineral Processing and Extractive Metallurgy 98, 123–131.

Das, S.C., 1996. Effect of Fe(II) during copper electrowinning at higher current density. International Journal of Mineral Processing 91–108.

Dew, D.W., Phillips, C.V., 1985a. The effect of Fe(II) and Fe(III) on the efficiency of copper electrowinning from dilute acid Cu(II) sulphate solutions with the Chemelec cell. Part I. Cathodic and anodic polarisation studies. Hydrometallurgy 14, 331–349.

Dew, D.W., Phillips, C.V., 1985b. The effect of Fe(II) and Fe(III) on the efficiency of copper electrowinning from dilute acid Cu(II) sulphate solutions with the Chemelec cell. Part II. The efficiency of copper electrowinning from dilute liquors. Hydrometallurgy 14, 351–367.

Jiricny, V., Evans, J.W., 1999. A study of the spouted-bed electrowinning of copper. Proceedings of the COPPER'99 International Conference, vol. 3, Electrorefining and Electrowinning, TMS, Phoenix, pp. 629.

Lee, J.C., 1993. Electrogenerative oxidation of ferrous ions with graphite electrodes. Journal of Applied Electrochemistry 23 (7), 745.

Marconi, P.F., Meunier, V., Vatistas, N., 1996. Recovery of pickling effluents by electrochemical oxidation of ferrous to ferric chloride. Journal of Applied Electrochemistry 26 (7), 693.

Peykova, M., Michailova, E., Stoychev, D., 1995. Galvanostatic studies of the nucleation and growth kinetics of copper in the presence of surfactant. Electrochimica Acta 40 (16), 2595–2601.

Rao, S.R., Finch, J.A., Kuyucak, N., 1995. Ferrous–ferric oxidation in acid mineral effluents: comparison methods. Minerals Engineering 8, 905–911.

Ronnholm, M.R., Warna, J., Salmi, T., 1999a. Kinetics of the oxidation of ferrous sulphate with molecular oxygen. Journal of Information in Chemical Engineering and Science 54 (19), 4223.

Ronnholm, M.R., Warna, J., Salmi, T., 1999b. Oxidation kinetics of ferrous sulphate over active carbon. Industrial and Engineering Chemical Research 38 (7), 2607.

Sandoval, S.P., 1995. A substitute anode for electrowinning copper. In: Cooper, W.C. (Ed.), Proceedings of the COPPER'95 International Conference, vol. III, Electrorefining and Hydrometallurgy of Copper, The Metallurgical Society of CIM, Toronto, pp. 423–435.

Vicenzo, A., Cavallotti, P.L., 2002. Copper electrodeposition from a pH 3 sulfate electrolyte. Journal of Applied Electrochemistry 32 (7), 743–753.

Zagorovskii, G.M., Prikhodko, G.P., Ogenko, V.M., 2001. Deposition of copper from dilute solutions onto disperse graphite cathode. Russian Journal of Applied Chemistry 74 (3), 424–426.